

# Kinetics and Mechanism of the Sonolytic Destruction of Methyl *tert*-Butyl Ether by Ultrasonic Irradiation in the Presence of Ozone

JOON-WUN KANG

Department of Industrial Environment & Health, Yonsei University, Wonju Campus, 234 Maeji, Wonju, Korea 220-710

MICHAEL R. HOFFMANN\*

W. M. Keck Laboratories, California Institute of Technology, Pasadena, California 91125

The kinetics and mechanism of the sonolytic degradation of methyl *tert*-butyl ether (MTBE) have been investigated at an ultrasonic frequency of 205 kHz and power of 200 W L<sup>-1</sup>. The observed first-order degradation rate constant for the loss of MTBE increased from  $4.1 \times 10^{-4} \text{ s}^{-1}$  to  $8.5 \times 10^{-4} \text{ s}^{-1}$  as the concentration of MTBE decreased from 1.0 to 0.01 mM. In the presence of O<sub>3</sub>, the sonolytic rate of destruction of MTBE was accelerated substantially. The rate of MTBE sonolysis with ozone was enhanced by a factor of 1.5–3.9 depending on the initial concentration of MTBE. *tert*-Butyl formate, *tert*-butyl alcohol, methyl acetate, and acetone were found to be the primary intermediates and byproducts of the degradation reaction with yields of 8, 5, 3, and 12%, respectively. A reaction mechanism involving three parallel pathways that include the direct pyrolytic decomposition of MTBE, the direct reaction of MTBE with ozone, and the reaction of MTBE with hydroxyl radical is proposed.

## Introduction

Since 1990, MTBE (methyl *tert*-butyl ether) has been used as a gasoline additive to reduce volatile organic carbon emissions from motor vehicles. However, the new gasoline additives such as MTBE have had negative environmental impacts on water quality due to leakage of petroleum products from the underground storage tanks. For example, MTBE, which is highly soluble (e.g., 0.35–0.71 M (1)), has been detected at high concentrations in groundwater. MTBE is reported to be resistant to both aerobic and anaerobic microbial degradation (2), and it is poorly adsorbed on granular activated carbon (GAC). In addition, due to its low volatility, air stripping is not a viable process for the removal of MTBE from water (1). Velleitner et al. (3) investigated the reaction of MTBE and O<sub>3</sub> in water, and they reported that 5.5 mol of ozone/mol of MTBE was required for 80% net destruction of MTBE. Barreto et al. (4) degraded MTBE photocatalytically and found that the degradation rate was significantly faster than the direct reaction between MTBE and O<sub>3</sub>.

Over the last several years, ultrasonic irradiation has been explored for the treatment of chemical contaminants in aqueous solution (5–10). The chemical effects of sonolysis are the direct result of the formation of cavitation microbubbles. The sonolytically induced microbubbles grow

with each successive ultrasonic frequency cycle until they reach a critical resonance frequency size that results in the violent collapse of gas bubbles. The rapid implosion of cavitation bubbles is accompanied by adiabatic heating of the vapor phase of the bubble that yields localized transient high temperature and pressure. Temperatures and pressures obtained upon bubble collapse have been estimated to be on the order of 4200 K and 975 bar, respectively (11). Temperatures exceeding 5000 K have been reported (12) in the ultrasonic cavitation of organic and polymeric liquids. Water vapor under these conditions undergoes a thermal dissociation to yield extremely reactive radicals, H<sup>•</sup> and OH<sup>•</sup>, and in the presence of O<sub>2</sub> yields HO<sub>2</sub><sup>•</sup>. As a result, organic compounds present near bubble/water interface can undergo thermal decomposition, and/or secondary reactions take place between solute molecules and the reactive radicals. Even though the basic physics and chemistry of reactions of cavitation are fairly well understood, many questions concerning detailed reaction mechanisms remain unanswered.

In particular, the combined process of ozonation and sonolysis needs to be explored further. Thus, the primary objective of this study is to determine the kinetics and mechanism of the sonolytic reaction of ozonation and sonolysis for the rapid degradation of MTBE in the aqueous solution.

## Experimental Methods

MTBE (99.9%; EM Science), *tert*-butyl formate (99%; Aldrich), *tert*-butyl alcohol (99%; EM Science), acetone (99.5%; EM Science), methyl acetate (99.5%; Aldrich), sodium bicarbonate (Reagent Grade; EM Science), and other chemicals were used without further purification.

The ultrasonic irradiations were performed with an Ultrasonic Transducer USW 51 (AlliedSignal ELAC Nautik, Inc.) in a glass and titanium reactor operating at 205 kHz with an active acoustic vibration area of 25 cm<sup>2</sup>. All reactions were performed in a 500-mL double-walled (cooling jacket) reaction chamber as described previously (7). The reactor had four sampling ports to withdraw aqueous samples and to allow gases to be introduced and vented. The interior diameter of the reaction vessel was 6 cm. Temperature was maintained constant at 20 °C throughout all kinetic runs.

Sonolyses were performed in water purified by a MilliQ UV Plus system ( $R > 18 \text{ M}\Omega$ ). Solutions containing O<sub>3</sub> were prepared by bubbling ozone that was generated via the corona discharge process on O<sub>2</sub> with an Orec ozonator (model V10-0) into deionized water at a flow rate of 100 mL min<sup>-1</sup> through a glass fritted diffuser until the desired aqueous-phase ozone concentration was obtained. The target aqueous ozone solution was monitored by UV spectrophotometry, using the molar extinction coefficient of 3300 M<sup>-1</sup> cm<sup>-1</sup> for O<sub>3</sub> in water at 254 nm (13).

All kinetic runs were made in the batch mode without adding a buffer. The initial pH values of the solutions were in the range of 6.6–6.8. MTBE stock solutions (100 mM) were prepared and stored at 4 °C until use. After being saturated, the ozone solutions were prepared, an appropriate volume of the MTBE stock solution was spiked into 500 mL of water saturated with ozone and was mixed with bubbling ozone gas for a few more seconds at a low flow rate to minimize any sparging effects. After the ozone supply valve was closed, the  $t = 0$  samples were taken, and the sonolytic irradiation was initiated. Typical irradiation intensity was at a power density at 200 W L<sup>-1</sup>. During each 60-min kinetic run, 1.0 mL of sample was taken at appropriate time intervals and stored in 20-mL Teflon-faced aluminum-sealed vials. In

\*To whom correspondence should be addressed. Phone: (818)395-4931; fax: (818)395-3170; e-mail: mrh@cco.caltech.edu.

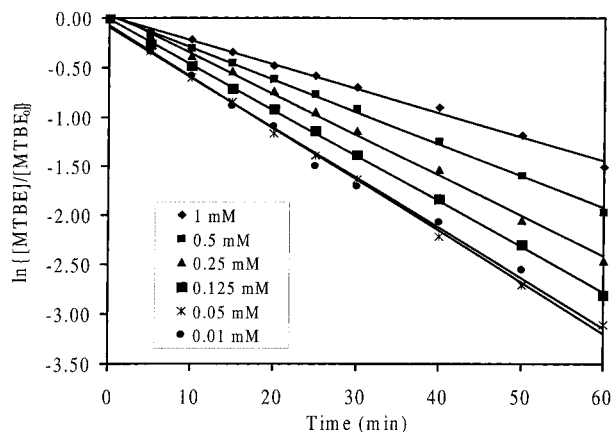


FIGURE 1. Pseudo-first-order plot for the destruction of MTBE by ultrasonic irradiation at 205 kHz,  $T = 20\text{ }^{\circ}\text{C}$ , and  $\text{pH}_0 = 6.6\text{--}6.8$ .

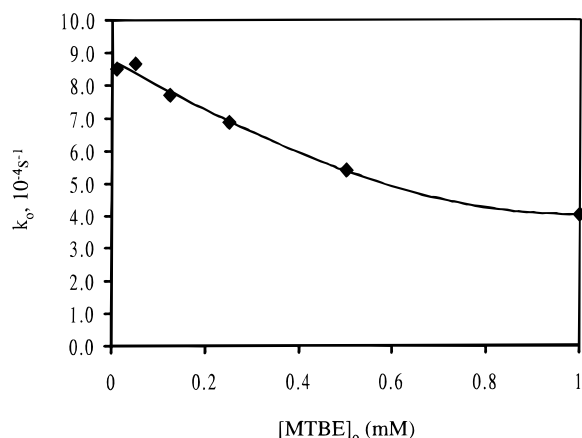


FIGURE 2. Variation of the pseudo-first-order rate constants ( $k_0$ ) with initial MTBE concentration ( $[\text{MTBE}]_0$ ).

ozonation runs, the residual aqueous ozone was quenched with 1 N  $\text{Na}_2\text{S}_2\text{O}_3$ . The total amount of samples withdrawn from the reactor was less than 15 mL, which introduced a small error ( $\leq 3\%$ ) due to differential volume changes ( $dV/dt$ ) during a given kinetic run.

MTBE and its identifiable oxidation byproducts were analyzed by gas chromatography. For the routine kinetic runs, compounds were analyzed by the headspace GC with FID detection. The compounds that were extracted into the gas phase of headspace sample in a HP 7694 headspace sampler were auto-injected into a HP 5890 series II GC-FID equipped with a HP-624 capillary column ( $30\text{ m} \times 0.32\text{ mm} \times 1.8\text{ }\mu\text{m}$ ) with  $70\text{ }^{\circ}\text{C}$  isothermal oven temperature for 10 min. Byproducts of MTBE were identified by injecting 100  $\mu\text{L}$  of the extracted headspace sample into a Hewlett-Packard 5890 series II gas chromatograph connected to a quadrupole-type mass spectrometer (HP 5989A) equipped with a HP-5MS capillary column ( $30\text{ m} \times 0.25\text{ mm} \times 1\text{ }\mu\text{m}$ ). The temperature ramp was programmed to  $30\text{ }^{\circ}\text{C}$  for 6 min and increased at  $10\text{ }^{\circ}\text{C}/\text{min}$  to  $150\text{ }^{\circ}\text{C}$ . Samples aliquots for hydrogen peroxide analysis were taken at 10-min intervals over a 60-min run time and were measured fluorometrically (14).

## Results and Discussion

First-order plots of  $\ln [\text{MTBE}]/[\text{MTBE}]_0$  vs time for representative kinetic runs are shown in Figure 1 in which the initial concentrations of MTBE (0.01–1.0 mM) were varied at a fixed power density of  $200\text{ W L}^{-1}$  and at a frequency of 205 kHz. A separate plot (Figure 2) of the pseudo-first-order rate constants,  $k_0$ , versus  $[\text{MTBE}]_0$  shows that  $k_0$  decreases with an increase in  $[\text{MTBE}]_0$ . On the basis of first-order

kinetics, the time required for 90% oxidation of MTBE is calculated to be 45 min (at a  $k_0$  of  $8.5 \times 10^{-4}\text{ s}^{-1}$ ) when the initial concentration was 0.01 mM; whereas, this time was increased to 93 min at a  $k_0$  rate of  $4.1 \times 10^{-4}\text{ s}^{-1}$  and at  $[\text{MTBE}]_0 = 1.0\text{ mM}$ . These results indicate that the observed reaction rate is limited either by diffusion of  $\text{OH}^{\bullet}$  out of the interfacial regions of the collapsing cavitation bubbles or by limited interfacial surface areas for chemical reaction between  $\text{OH}^{\bullet}$  and MTBE.

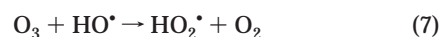
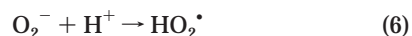
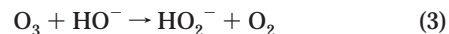
Since  $\text{CO}_3^{2-}$  and  $\text{HCO}_3^-$  are potential competitive reagents for  $\text{OH}^{\bullet}$ , the effect of  $[\text{HCO}_3^-]$  on the oxidation rate of MTBE was investigated. Glaze and Kang (15) reported that high levels of bicarbonate ion (e.g., 1–4 mM) in groundwater significantly decreased the rate of removal of TCE and PCE during UV-ozonolysis because of competitive reaction  $\text{OH}^{\bullet} + \text{HCO}_3^- \rightarrow \text{H}_2\text{O} + \text{CO}_3^{\bullet-}$ . The second-order rate constants of  $\text{OH}^{\bullet}$  with bicarbonate ion ( $k = 1.5 \times 10^7\text{ M}^{-1}\text{s}^{-1}$ ) (16) and MTBE ( $k = 1.57 \times 10^9\text{ M}^{-1}\text{s}^{-1}$ ) (17) are nearly identical. However, the effects of a variation of the concentration  $\text{HCO}_3^-$  on the rate of sonolytic degradation of MTBE were found to be negligible over a range of  $[\text{HCO}_3^-]$  from 1 to 2 mM. This result suggests that the major reaction site for MTBE with  $\text{OH}^{\bullet}$  is in the vapor phase of the cavitating bubbles within the super hot interfacial region between the vapor and surrounding liquid phases but not in the bulk aqueous phase.

The enhancement in the apparent rates of organic compound degradation via the coupling of ultrasound and ozone has been investigated previously (6, 18, 19). For example, Hua and Hoffmann (6) reported that the presence of ozone during sonolysis at 20 kHz did not enhance the rate of carbon tetrachloride destruction; however, they showed that the combined process of ozone and sonication did reduce the accumulation of intermediates and byproducts. However, Barbier and Petrier (20) showed that the combined ozone-ultrasound process was capable of complete mineralization of 4-nitrophenol. In the bulk aqueous phase, ozone can be decomposed by hydroxide ion,  $\text{OH}^-$ , or the conjugate base of  $\text{H}_2\text{O}_2$  ( $\text{HO}_2^-$ ) to yield  $\text{HO}_2^{\bullet}$  and  $\text{OH}^{\bullet}$ . Both direct reactions with  $\text{O}_3$  and indirect reaction with its free radical decomposition products can occur in aqueous solution.

During acoustic cavitation, water is pyrolytically decomposed leading to the formation of hydroxyl and hydroperoxyl radicals as follows (7):

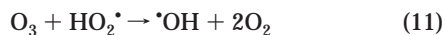


In the bulk aqueous phase, ozone can be decomposed by hydroxide ion,  $\text{OH}^-$ , or the conjugate base of  $\text{H}_2\text{O}_2$  ( $\text{HO}_2^-$ ) to yield  $\text{HO}_2^{\bullet}$  and  $\text{OH}^{\bullet}$  as shown below:

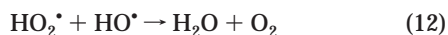




Since hydrogen peroxide has been shown to form during the sonolysis of water (7), the coupled reactions of ozone and hydrogen peroxide will also contribute to the overall observed reactivity with organic compounds as follows:



The above series of elementary reactions constitute a free radical chain reaction leading to the degradation of ozone and the formation of hydroxyl and hydroperoxyl radicals as reactive intermediates. The chain termination steps are as follows:



During our previous experiments (7), we followed the production of hydrogen peroxide due to this latter termination reaction and due to the self-reaction of two hydroperoxyl radicals.

Ozone can react in aqueous solution either directly with target substrates or indirectly via reactions with its free radical decomposition products. In the ozone-ultrasound process, however, ozone most likely decomposes in the gas phase of the cavitation bubbles by a thermal process that yields oxygen atoms and oxygen:



Thus, a wide variety of reactions may also be expected to occur directly in the gas phase of cavitation bubbles.

The effects of ozone ( $[\text{O}_3]_0 = 0.26\text{--}0.34\text{ mM}$ ) coupled with ultrasonic irradiation on the rate of MTBE degradation were investigated at several differential initial MTBE concentrations (0.01–1.0 mM) at a fixed sonolytic input power. These results (Figure 3), which are summarized in Table 1, showed that simple addition of  $\text{O}_3$  to the influent oxygen gas during sonolysis accelerates the degradation of MTBE by a factor of 1.5–3.9, depending on the initial concentration of MTBE. These results also show that MTBE degrades very slowly by ozonation alone under ambient conditions. However, the direct reaction of MTBE with ozone appears to be enhanced at the cavitation bubble interface due to zones of higher temperature or due to indirect reactions with ozone decomposition products. In Table 2, a direct comparison of the pseudo-first-order rate constants, which were obtained for various initial reaction conditions, is provided with the corresponding reaction half-lives.

As described above,  $\text{H}_2\text{O}_2$  is produced during the sonolysis of water (7, 21). The rate of hydrogen peroxide production during sonolysis can be expressed as follows:

$$\frac{d[\text{H}_2\text{O}_2]}{dt} = 2k_1[\cdot\text{OH}][\cdot\text{OH}] + 2k_2[\text{HO}_2\cdot][\text{HO}_2\cdot] - k_3[\cdot\text{OH}][\text{H}_2\text{O}_2] - k_{\text{pyr}}[\text{H}_2\text{O}_2] \quad (16)$$

where the first and the second terms on the right-hand side of eq 16 give the rate of the self-reactions of  $\text{OH}\cdot$  and  $\text{HO}_2\cdot$  to form  $\text{H}_2\text{O}_2$  ( $k_1 = 5.5 \times 10^9\text{ M}^{-1}\text{s}^{-1}$  (22),  $k_2 = 8.3 \times 10^5\text{ M}^{-1}$ ,

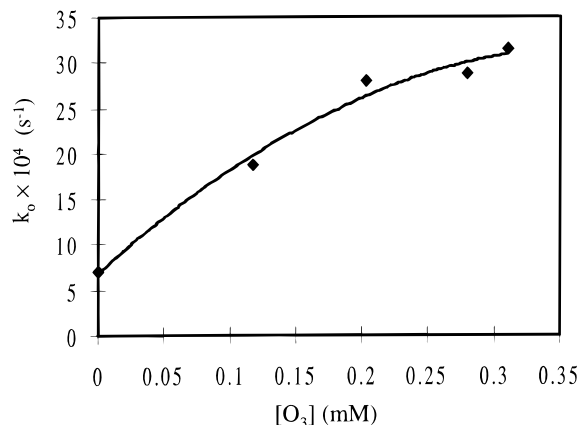


FIGURE 3. Effects of ozone on the pseudo-first-order rate constants for MTBE destruction at 205 kHz,  $T = 20^\circ\text{C}$ , and  $\text{pH}_0 = 6.6\text{--}6.8$ .

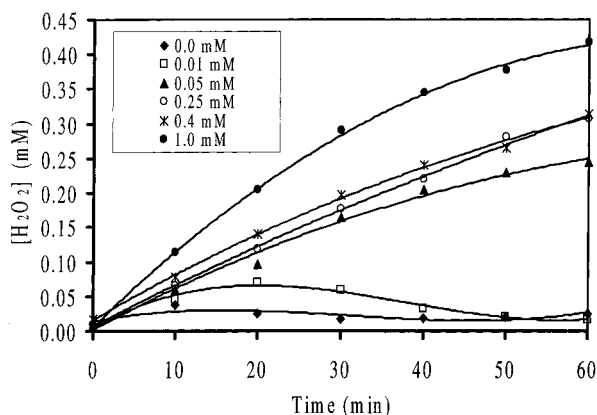


FIGURE 4. Effect of ozone on the hydrogen peroxide formation rate for the ultrasonic irradiation process at 205 kHz,  $T = 20^\circ\text{C}$ ,  $\text{pH}_0 = 6.6\text{--}6.8$ , and  $[\text{O}_3]_0 = 0.25\text{--}0.33\text{ mM}$ .

TABLE 1. Enhancement Effect of Ozone on the Pseudo-First-Order Rate Constants for Ultrasonic Degradation of MTBE at 205 kHz and at  $20^\circ\text{C}$

[MTBE] <sub>0</sub> (mM)	[O <sub>3</sub> ] (mM)	$k_0$ ( $10^{-4}\text{s}^{-1}$ )		$E^a$
		ultrasound	O <sub>3</sub> + ultrasound	
0.01	0.30	8.5	33.2	3.9
0.05	0.31	8.7	31.3	3.6
0.25	0.32	6.9	14.9	2.2
0.50	0.34	5.4	12.2	2.3
1.00	0.26	4.1	6.3	1.5

<sup>a</sup> Enhancement factor =  $k_0(\text{ozone} + \text{ultrasound})/k_0(\text{ultrasound alone})$ .

TABLE 2. Comparison of Pseudo-First-Order Rate Constants for Various Initial Conditions in 500-ml Sonochemical Reactor

conditions <sup>a</sup>	[O <sub>3</sub> ] or [O <sub>2</sub> ] (mM)	[MTBE] <sub>0</sub> (mM)	power (W L <sup>-1</sup> )	$k_0$ (s <sup>-1</sup> )	$t_{1/2}$ (min)
O <sub>2</sub> + US	0.25	0.05	200	$8.7 \times 10^{-4}$	13.3
O <sub>3</sub> + US	0.31	0.05	200	$31.3 \times 10^{-4}$	3.7
O <sub>2</sub> + no US	0.25	0.70	NA <sup>b</sup>	≈0	NA
O <sub>3</sub> + no US	0.25	0.31	NA	$0.6 \times 10^{-4}$	192

<sup>a</sup> US, ultrasound. <sup>b</sup> NA, not applicable.

$\text{s}^{-1}$  (22), the third term reflects the reaction of  $\text{OH}\cdot$  radicals with  $\text{H}_2\text{O}_2$  ( $k_3 = 2.7 \times 10^7\text{ M}^{-1}\text{s}^{-1}$  (23)), and  $k_{\text{pyr}}$  reflects the rate of degradation of  $\text{H}_2\text{O}_2$  due to direct pyrolysis at elevated temperatures.

The effects of variable [MTBE] and  $[\text{O}_3]$  on the rate of hydrogen peroxide production,  $d[\text{H}_2\text{O}_2]/dt$ , showed a net linear increase in  $[\text{H}_2\text{O}_2]$  with sonication time (i.e., zero-

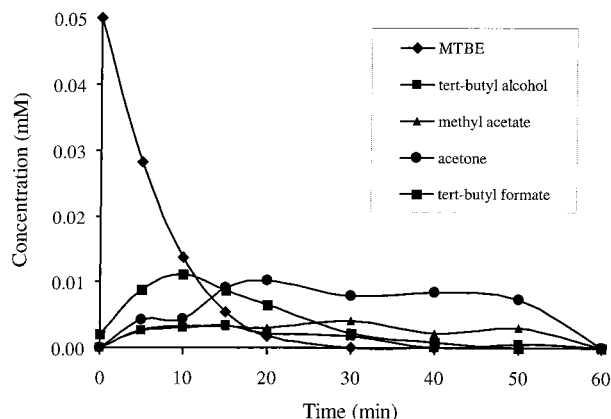
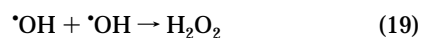


FIGURE 5. MTBE degradation and its byproducts formation profiles by ozone-ultrasound process at at 205 kHz,  $T = 20\text{ }^{\circ}\text{C}$ ,  $\text{pH}_0 = 6.6\text{--}6.8$ ,  $[\text{MTBE}]_0 = 0.5\text{ mM}$ , and  $[\text{O}_3]_0 = 0.25\text{ mM}$ .

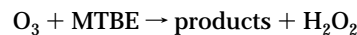
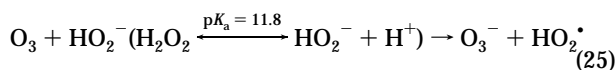
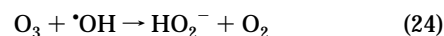
order with observed rates over the range of  $1.5\text{--}2.1\text{ }\mu\text{M min}^{-1}$ ). However, the  $\text{H}_2\text{O}_2$  formation rate appeared to decrease with an increase in the initial concentration of MTBE. The decreased rate of peroxide formation is most likely due to the competitive reaction of MTBE with  $\text{OH}^{\bullet}$  in the cavitation bubble. For example, at higher  $[\text{MTBE}]_0$ , smaller steady-state  $[\text{OH}^{\bullet}]$  values are likely to be obtained due to the reaction of MTBE with  $\text{OH}^{\bullet}$  (e.g.,  $\text{MTBE} + \text{OH}^{\bullet} \rightarrow k_{\text{MTBE,OH}} = 1.57 \times 10^9\text{ M}^{-1}\text{ s}^{-1}$ ). In a second set of experiments, the effect of ozone on the peroxide formation rate was investigated by varying the initial MTBE concentration at a fixed initial ozone concentration ( $0.29\text{ mM}$ ). The  $[\text{H}_2\text{O}_2]$  vs time profiles (Figure 4) showed that with higher  $[\text{MTBE}]_0$ , larger rates of  $\text{H}_2\text{O}_2$  production were obtained, and when  $[\text{MTBE}]_0 \geq 0.05\text{ mM}$ , more  $[\text{H}_2\text{O}_2]$  is produced from the combined  $\text{O}_3$ -ultrasound system than from the ultrasonic system alone. This effect may be attributed to  $\text{H}_2\text{O}_2$  production via reactions involving the intermediates of MTBE degradation. In addition, the fastest initial rate of  $\text{H}_2\text{O}_2$  production occurred in a  $1\text{ mM}$  solution of MTBE that did not appear to follow simple zero-order kinetics. The resultant shape of the kinetic curve indicates that the relative contribution of the second term of eq 16 (i.e., the quenching of  $\text{OH}^{\bullet}$  by peroxide) is greater as  $\text{H}_2\text{O}_2$  accumulates in solution during sonolysis. Furthermore, the lowest rates of production of hydrogen peroxide occurred during sonolysis at lower initial concentrations of MTBE ( $[\text{MTBE}]_0 = 0.01\text{ mM}$ ) and in MTBE-free water as shown in Figure 4.

Several possible mechanisms may account for the above observations. In mechanism I shown below,  $\text{O}_3$  decomposes via pyrolysis in the cavitation bubbles to yield oxygen atoms and an elevated steady-state level of hydroxyl radical,  $[\text{OH}]_{\text{ss}}$ .

#### mechanism I



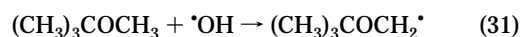
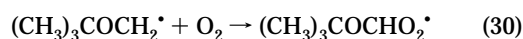
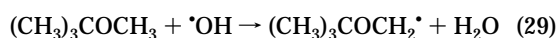
#### mechanism II



As a consequence, a higher concentration of  $\text{H}_2\text{O}_2$  than was observed should have been obtained. However, results shown in Figure 4 are not consistent with mechanism I. However, mechanism II, which is illustrated above, may provide a more plausible explanation for the observed trends in reactivity. In mechanism II, ozone reacts with  $^{\bullet}\text{OH}$  and with the conjugate base of  $\text{H}_2\text{O}_2$  ( $\text{HO}_2^-$ ) at the cavitating bubble interfaces.

As noted above, the combined  $\text{O}_3$ -ultrasound system is much more effective in degrading MTBE than either the ultrasound or the  $\text{O}_3$  systems alone. This apparent combinatory effect may be attributed to the direct reaction of ozone and MTBE at the cavitation bubble interfaces. The direct reaction rate of ozone with MTBE is very slow under the ambient conditions, but its reaction rate may be substantially enhanced at the higher temperatures of the interfacial regions of the cavitating bubbles (4).

To further explore the reaction mechanism of MTBE degradation during the  $\text{O}_3$ -ultrasound process, several intermediates and byproducts of the oxidative degradation of MTBE were identified by GC/MSD. *tert*-Butyl formate (TBF), *tert*-butyl alcohol (TBA), methyl acetate (MA), and acetone were major intermediates identified by GC/MSD after injection of headspace gas samples. The subsequent concentrations were quantified by using the GC/FID. In a sonicated solution of MTBE ( $0.05\text{ mM}$ ), TBF was produced immediately and reached its highest concentration ( $[\text{TBF}] = 0.011\text{ mM}$ ) after 10 min of irradiation. After 40 min of irradiation, all traces of TBF were eliminated as shown in Figure 5. At the same time, methyl acetate and acetone were formed and remained at steady-state levels with average yields of 3% and 12%, respectively. However, after 60 min of continued irradiation both methyl acetate and acetone were also eliminated. Lower steady-state concentrations of TBA were produced. TBA and acetone were formed after the production of TBF. These observations suggest that TBF is the initial intermediate product of MTBE oxidation as follows:





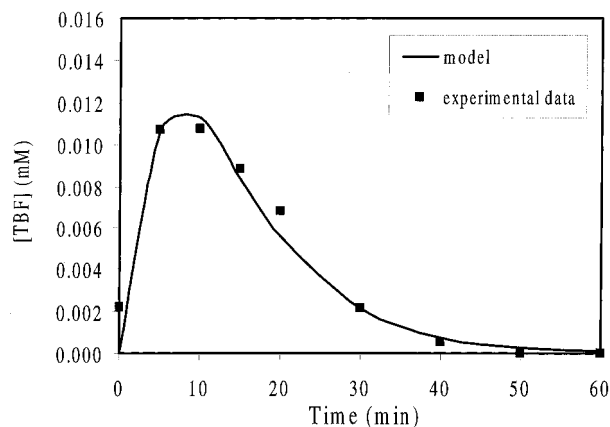


FIGURE 7. Comparison between measured and predicted of *tert*-butyl formate concentration with ozone–ultrasound system at 205 kHz,  $T = 20\text{ }^{\circ}\text{C}$ ,  $\text{pH}_0 = 6.6\text{--}6.8$ ,  $[\text{MTBE}]_0 = 0.5\text{ mM}$ , and  $[\text{O}_3]_0 = 0.25\text{ mM}$ .

$$[\text{TBF}]_t = \left( \frac{\eta k_o [\text{MTBE}]_0}{k_{\text{TBF,II}} - k_o} \right) \left[ \frac{\exp\{(k_{\text{TBF,II}} - k_o)t\} - 1}{\exp(k_{\text{TBF,II}}t)} \right] \quad (41)$$

The parameter  $\eta$  is estimated by fitting the predicted values of [TBF] based on eq 41 to the experimental data. The best fit for the experimental data is given by  $\eta = 0.53$ . This indicates that 53% of MTBE is degraded via mechanism II. Figure 7 shows that the agreement between the simple kinetic model and the experimental data is excellent.

The results of this study demonstrate that the combination of ozonation and sonication (i.e.,  $\text{O}_3$ –ultrasound system) can effectively degrade MTBE into innocuous and biodegradable products. The combined  $\text{O}_3$ –ultrasound process may provide a suitable alternative in future for the elimination of MTBE from contaminated groundwater.

### Acknowledgments

Support for this research has been provided by the Department of Energy (DOE Grant 1-963472402) via Argonne National Laboratory.

### Literature Cited

- (1) Mackay, D.; Shiu, W.-Y.; Ma, K.-C. *Illustrated Handbook of Physical–Chemical Properties and Environmental Fate for Organic Chemicals (Vol. III)*; Lewis Publishers: Chelsea, MI, 1993.
- (2) Suffita, J. M.; Mormile, M. R. *Environ. Sci. Technol.* **1993**, *27*, 976–978.
- (3) Velleitner, N. K.; Papillhou, A. L.; Croue, J. P.; Peyrot, J.; Dore, M. *Ozone Sci. Eng.* **1994**, *16*, 41–54.
- (4) Barreto, R. D.; Gray, K. A.; Anders, K. *Water Res.* **1995**, *29*, 1243–1248.
- (5) Hua, I.; Hochemer, R. H.; Hoffmann, M. R. *J. Phys. Chem.* **1995**, *99*, 2335–2342.
- (6) Hua, I.; Hoffmann, M. R. *Environ. Sci. Technol.* **1996**, *30*, 864–871.
- (7) Hua, I.; Hoffmann, M. R. *Environ. Sci. Technol.* **1997**, *31*, 2237–2243.
- (8) Kotronarou, A.; Mills, G.; Hoffmann, M. R. *Environ. Sci. Technol.* **1992**, *26*, 2420–2428.
- (9) Kotronarou, A.; Mills, G.; Hoffmann, M. R. *J. Phys. Chem.* **1991**, *95*, 3630–3638.
- (10) Serpone, N.; Hidaka, H.; Pelizzetti, E. *J. Phys. Chem.* **1994**, *98*, 2634–2640.
- (11) Mason, T.; Lorimer, J. P. *Sonochemistry: Theory, Applications, and Uses of Ultrasound in Chemistry*; Ellis Norwood. Ltd.: Chichester, U.K., 1988.
- (12) Flint, E. B.; Suslick, K. S. *Science* **1991**, *253*, 1397–1399.
- (13) Glaze, W. H.; Kang, J.-W.; Chapin, D. H. *Ozone: Sci. Eng.* **1987**, *9*, 335–352.
- (14) Lazrus, A. L.; Kok, G. L.; Gitlin, S. N.; Lind, J. A. *Anal. Chem.* **1985**, *57*, 917–922.
- (15) Glaze, W. H.; Kang, J.-W. *J. Am. Water Works Assoc.* **1988**, *80*, 57–63.
- (16) Weeks, J. L.; Rabani, J. *J. Phys. Chem.* **1966**, *70*, 2100.
- (17) Atkinson, R. *Chem. Rev.* **1985**, *85*, 69–201.
- (18) Hart, E. J.; Henglein, A. J. *J. Phys. Chem.* **1986**, *90*, 3061–3062.
- (19) Olson, T. M.; Barbier, P. F. *Water Res.* **1994**, *28*, 1383–1391.
- (20) Barbier, P. F.; Petrier, C. *J. Adv. Oxid. Technol.* **1996**, *1*, 154–159.
- (21) Ficher, C.-H.; Hart, E. J. *J. Phys. Chem.* **1986**, *90*, 3059–3060.
- (22) Buxton, G. V.; Greenstock, C. L.; Helman, W. P.; Ross, A. B. *J. Phys. Chem. Ref. Data* **1988**, *17*, 513–886.
- (23) Christensen, H. S.; Sehested, H.; Corfitzan, H. *J. Phys. Chem.* **1982**, *86*, 15–88.

Received for review October 3, 1997. Revised manuscript received July 1, 1998. Accepted July 21, 1998.

ES970874U